IJICIS, Vol.23, No.3, 9-18
DOI: 10.21608/ijicis.2023.189590.1250

International Journal of Intelligent Computing and Information Sciences

https://ijicis.journals.ekb.eg/

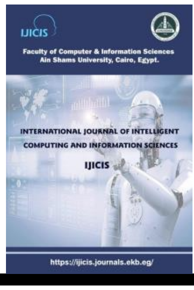

DETECTION OF ORBITAL TUMORS ON MRI IMAGES USING CONVOLUTIONAL NEURAL NETWORKS

Esraa Allam*

Computer Science Department,
Faculty of Computer and Information Sciences, Ain Shams University,
Cairo, Egypt
esraa.allam@gmail.com

Marco Alfonse

Computer Science Department,
Faculty of Computer and Information Sciences, Ain Shams University,
Cairo, Egypt
marco_alfonse@cis.asu.edu.eg

Abdel-Badeeh M. Salem

Computer Science Department
Faculty of Computer and Information Sciences, Ain Shams University,
Cairo, Egypt
abSalem@cis.asu.edu.eg

Received 2023-01-25; Revised 2023-07-01; Accepted 2023-07-10

Abstract: *Orbital tumors are the most common type of tumor affecting the orbit. Some factors, such as technical causes relating to imaging quality and human error, contribute to radiologists misdiagnosing eye tumors. Computer-aided detection systems (CADs) are being developed to address these limitations and have recently been used in numerous imaging modalities for eye tumor diagnosis. CAD technologies increase radiologists' ability to detect and distinguish between normal and diseased tissues. These techniques are only conducted as a second opinion, but the radiologist makes the final decisions. This article presents the contemporary CAD method for detecting orbital tumors on magnetic resonance imaging (MRI) utilizing Convolutional Neural Networks (CNN). Pre-processing, Data Augmentation, Classification, and Evaluation are the four stages that involve our CAD system. Two datasets were used for MRI images: 1404 MRI T1-weighted images and 1560 MRI T2-weighted images. The system was evaluated by many evaluation metrics including the recognition rate which gives 95% for T1-weighted images and 94% for T2-weighted images.*

Keywords: *Artificial Intelligence, Deep Learning, Orbital Tumor, Image Classification, Medical Informatics.*

1. Introduction

The orbital tumor is a rare tumor that appears around the eye. It represents approximately 0.1% of all body tumors and approximately one-fifth of all orbit diseases [1]. It refers to any tumor found in the orbit, the bony socket in the front of the skull that holds the eye. Orbit tumors are irregular growths of lesions in the structure around the eye. It can be benign or malignant. Tumors involving the orbit are divided into; primary and secondary tumors. The primary tumors include cysts, vascular lesions, lymphomas and neurogenic tumors (arising from nerves). The secondary tumors called metastasizes include cancer that develops from another part and spreads to the orbit. Most patients with orbital tumors suffer eyeball bulging or double vision (diplopia) and a feeling of pressure in the eye. Pain can

***Corresponding Author**: Esraa Allam

Computer Science Department, Faculty of Computer and Information Science, Ain Shams University, Cairo, Egypt

Email address: esraa.allam@gmail.com

be caused by infections, inflammations, and some orbital malignancies [2]. Imaging examinations are required for detecting and diagnosing orbit tumors. Both approaches include magnetic resonance imaging (MRI) and computed tomography (CT) scans [3]. MRI images are recommended in general because they offer a better image of the components within the orbit. A biopsy may also be performed to analyze the tumor tissue under a microscope to obtain a clear diagnosis. MRI has two types of weighted images; T1-weighted and T2-weighted images [4].

We have observed the rise of computer science in disease detection and diagnosis for biological sciences during the previous many decades [5]. Artificial intelligence (AI) has transformed disease diagnosis, identification, classification, segmentation and anatomization by accomplishing categorization stages that were traditionally time-consuming and tiresome for specialists [6]. The medical industry has been adopting and implementing AI due to the recent surge in medical applications utilizing AI-based technology and clinicians' desire to operate with fewer mistakes, accidents, and misdiagnoses. Many AI and subclass Deep Learning (DL) networks are beneficial in medical image processing for the prognosis and diagnosis of many maladies; including breast, lung, and brain tumors, which are arduous and prone to human mistakes if handled manually. These DL techniques are used to process medical images in order to accomplish different tasks; including classification, detection, segmentation, localization, prediction and registration, effectively avoiding human abilities [7].

The application of AI in eye sickness detection and treatment is considerable [8]. The technique mandates accurate determination and isolation of ocular layers, allowing ophthalmologists to concentrate on treatment. The benefits of AI were used in this work to classify and diagnose orbital tumors. The proposed system is developed to identify and classify orbital tumors from MRI images. The images implement preprocessing and data augmentation to increase the model's performance and accuracy. Furthermore, the use of powerful AI systems in medical diagnostics and image identification has made considerable required progress in medical science. The automatic diagnosis of ocular tumors includes preprocessing using image normalization, categorization and sampling approaches, training neural networks with enormous volumes of data, and statistical analysis [9]. The researchers are now working on enhancing the accuracy of tumor classification and diagnosis, lowering computing time and memory use, correcting ocular layer segmentation, and minimizing computational complexity [10].

The most extensively used and powerful DL model for medical image processing is the convolutional neural network (CNN). CNNs enable a share leap in image comprehension by performing image classification, detection, segmentation, localization, and other tasks [11]. The effectiveness of CNNs in image interpretation is the primary reason for their widespread adoption. A CNN's design can aid in multilevel hierarchical feature learning [12]. The early layers can extract low-level characteristics, while the deep layers extract high-level semantic characteristics, which are then merged to reliably find important spots. The CNN demands the design more sensibly since the input is an image. The CNN architecture comprises an input layer, convolutional layer, rectified linear unit (ReLu), pooling layer, fully connected layer, and output layer. These layers are layered to form the CNN structure. The convolutional, ReLU, and pooling layers are used to extract features. Classification takes place in the fully connected layer [13].

The Convolution layer is designed to extract the image features such as edges, texture, and gradient direction from neural cells. Convolutional filters, or kernels, of size nxmxd, where d is the image depth, are used to create convolution layers. Intuitively, CNN learns filters that are triggered when it encounters edge, color, texture, and so forth. Its output is passed into an activation function layer. The pooling layer down samples the convolved features nonlinearly. Through dimensionality reduction, it reduces the computer power necessary to process the data. The pooling operation divides the input into a collection of rectangular patches. Depending on the type of pooling used, each patch is replaced with a single value. The last layer is the fully connected layer, in which each node has inbound connections from all inputs and all connections are weighted. Its output is the total of all inputs multiplied by weights that converted the input into a vector or one-dimensional array. It is followed by the sigmoid activation function, which completes the classifier task [12].

In this paper, a CAD system for detecting orbital tumors is presented. Our contribution is a construction of an intelligent system for identifying orbital tumors from MRI images using CNN. The following is how the rest of this paper is organized: The related work is described in section 2. The suggested system is described in section 3. Section 4 contains the findings of the experiments as well as a discussion. Section 5 contains the conclusion as well as the scope of future efforts.

2. Related Work

There are many studies on the classification of Eye tumors. Biswarup et al. [14] presented a system for classifying eye melanoma in medical images. The system is divided into three steps; images pre-processing step, images marked as tumors or not by medical experts and classification. In preprocessing steps, images were rescaled, cropped in the eye image's central portion, and resized the area proportionally. Then, the images were marked as melanoma or non-melanoma by medical experts. In the classification step, CNN is used as the classifier. A CNN comprises two convolutional layers and two sub-sampling layers, followed by three fully connected layers. The dataset is collected from New York Eye Cancer Center database. It consists of 170 images; 110 are eye melanoma and 60 are normal images. Ophthalmologists verified the proposed system, which obtained 91.76 % accuracy.

Sheshang et al. [15] established a system to determine eye melanoma in medical images. The system's four steps are preprocessing, segmentation and identification. Image preprocessing methods such as greyscale transformation for the images and median filter were applied. Otsu segmentation was applied as a thresholding method to images during the segmentation step to transform them into binary images. CNN is applied as a classifier during the classification step. A CNN consists of four convolutional layers and four maximum pooling layers, followed by two fully connected layers. The dataset is collected from two public websites "Miles Research" [16] and "Eye Cancer" [17]. The dataset consists of 200 images. The system was examined on its capacity to correctly detect eye melanoma at a high rate of 92.5%.

Parmod et al. [18] developed a classification system for recognizing retinoblastoma from fundus images. Segmentation and classification are the two steps of the system. The Otsu multi-thresholding technique was applied to segment the tumors from the fundus images. The next step was to classify the retinoblastoma in fundus images; this classification was carried out using two deep learning techniques AlexNet and ResNet50 algorithms. The dataset is obtained from an online website called MathWorks [19] with a total of 278 fundus images. The system recognized retinoblastoma with 93.16% for the ResNet50 algorithm and 88.12% for the AlexNet algorithm accuracy rate.

3. The Proposed System

This section depicts the pipeline used to implement our proposed system. The pipeline is divided into several stages, beginning with image acquisition, image preprocessing, image argumentation, model training and ending with model evaluation. Each step's output is utilized as input for the next stage in the pipeline. Figure 1 depicts the proposed model's pipeline.

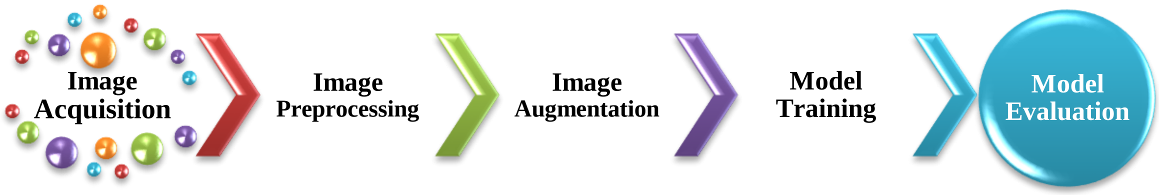

Figure. 1: Proposed approach pipeline

2.1. Image acquisition

Two datasets are utilized in conjunction with two types of magnetic resonance imaging (MRI): T1-weighted and T2-weighted images. There are 133 T1-weighted images in total; 20 normal images and 113 orbit tumor images. T2-weighted images tot 109 MRI images; 24 normal images and 85 orbit tumor images. Both tumor images were obtained from Ain Shams University Hospital, Ophthalmology Department. The normal images that are utilized in our experiments were manually obtained from various sources on the internet [20]. The tumor databases include 30 patients with various orbit tumor types. T1-weighted image dimension is (800 x 600) pixel resolution for the tumor image and the normal image is (509 x 400) pixel resolution. The tumor T2- weighted image dimension is (824 x 800) pixel resolution and the normal image is (516 x 471) pixel resolution. Figure 2 shows the different MRI image samples used in the experiment.

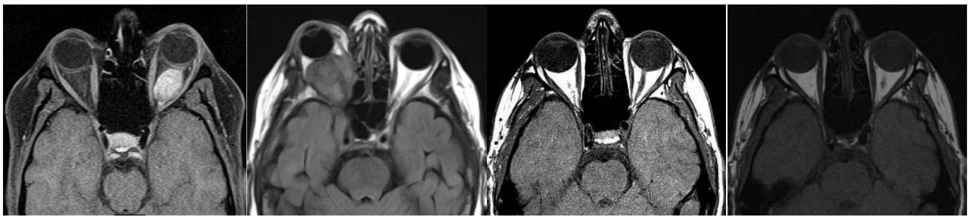

Normal T1-weighted Image Orbit tumor T1-weighted Image

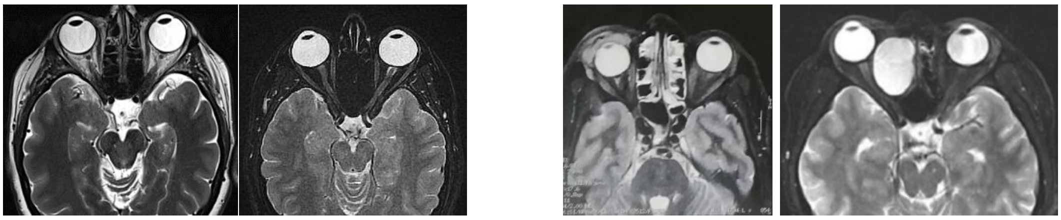

Normal T2-weighted Image Orbit tumor T2-weighted Image

Figure. 2: Sample of MRI image (Normal and Orbit tumor)

2.2. Image Preprocessing

Datasets in our work have insufficient data to employ in the training phase with a total size of T1-weighted images are 133 MRI images and T2-weighted images are 109 MRI images. The resampling approaches were applied to avoid overfitting in the experiment. First, the Oversampling approach was employed for each type of MRI image (normal and tumor) to increase the number of images utilized in categorization. Images were processed using the Gaussian blur filter, Median filter, Unsharp mask filter with radius size (0.5, 1, 2, and 3), sharpness filter with factor (0.5, 1, 1.5, 2, 3, and 4), EDGE Enhance Filter, EDGE Enhance More Filter, Brightness Filter with factor (0.5), and Contrast Filter with factor (0.5) for normal type. Images were processed using the median filter, sharpness filter with factors (0.5, 1, 3, and 4) and Unsharp Mask filter with radius size (1.5) for tumor type. The total size of T1-weighted images is 702 MRI images, whereas the total size of T2-weighted images is 780 MRI images. Second, divide the datasets in our experiment into training, validation, and testing sets using an 80/20 method; 10% is validation and 10% is testing. The 80-20 split ratio is a typical ratio in deep learning and has been applied in medical images [21]. Figure 3 depicts examples of MRI T1-weighted images after the image filter had been applied. Figure 4 depicts examples of MRI T2-weighted images after the image filter had been applied.

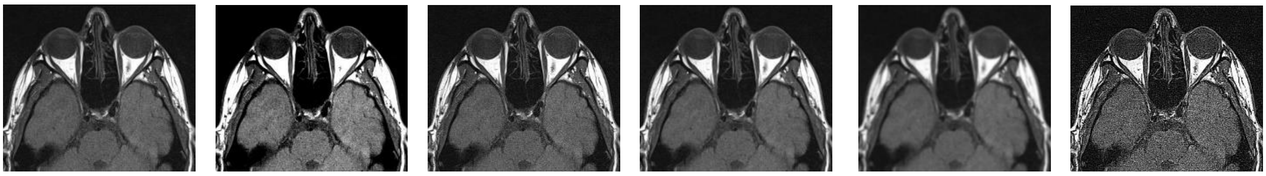

Original Image Contract filter Sharpness filter Median filter Gaussian blur filter Edge enhance filter

Normal T1-weighted images

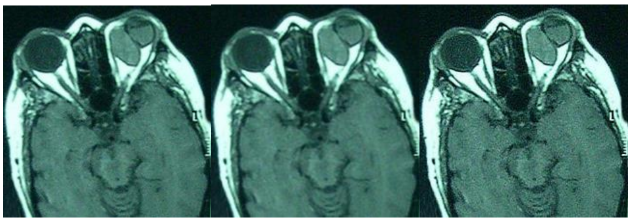

Original Image Median filter Sharpness filter

Tumor T1-weighted images

Figure. 3: Sample of MRI T1-weighted images with filter (Normal and Orbit tumor)

2.3. Image Augmentation

Many clinical imaging collections are uneven, making it difficult to find a substantial quantity of data for a single clinical instance. Skewed data distribution is a common issue in medical image categorization difficulties. Data augmentation is one way to deal with inadequate training data. Data augmentation expands a dataset by rescaling, resizing, and rotating existing data at the runtime to create new images while preserving the same label. On larger datasets, deep learning special CNN models outperform. Augmenting images increases the total quantity of images which allows the model to train more effectively [22]. Data Augmentation is also considered a type of dataset-level regularization since it reduces over-fitting and improves generalization performance by enriching the training dataset itself, which is the source of the problem. Additionally, it is utilized to overcome the issue of an imbalanced class by oversampling the minority class to enlarge the dataset and make the model perform better on the training data [23].

The dataset in the experiment includes small samples, and data augmentation was performed to enhance the number of these data. We used geometric transformation techniques on the MRI images to prevent over-fitting during the training phase. First, the images were resized to 224 x 224 pixels in width and height. Second, the images were rescaled so that the pixel range changes from [0, 255] to [0, 1]. Third, the images were rotated by 40° degrees. Fourth, the images had shifted the width and height by 20%. Fifth, the images were sheared by 20%. Seventh, the images were zoomed in 20%. Finally, the images were flipped horizontally, reflecting the central horizontal axis.

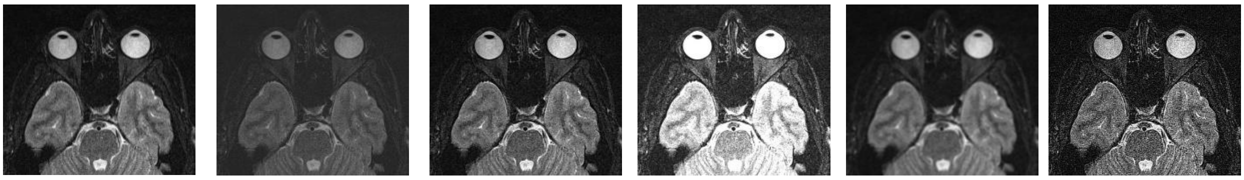

Original Image Contract filter Sharpness filter Brightness filter Gaussian blur filter Edge enhance filter

Normal T2-weighted images

Original Image Median filter Sharpness filter

Tumor T2-weighted images

Figure. 4: Sample of MRI T2-weighted images with filter (Normal and Orbit tumor)

2.4. The Architecture of the CNN Model

Our CNN model architecture is divided into eight layers. It was trained with 80 epochs and 64 batch sizes. Figure 5 shows the CNN model architecture. The eight network layers are as followed: a first convolutional layer followed by a first max pooling layer, a second convolutional layer followed by a second max pooling layer, and a flattered layer followed by two fully connected layers. The convolutional layer worked well as a feature extraction layer because it deals with spatial redundancy via weight sharing, resulting in a feature map; the output of this layer identifies fundamental features such as straight edges and corners. The pooling layer decreases the feature map's dimensionality while keeping the most critical elements. As a result, the number of parameters to learn and the quantity of computation performed in the network is reduced. It summarizes the properties of a convolution layer-formed feature map area. The flattened layer reshapes the preceding layer's output and generates a one-dimensional vector as an input to a fully connected layer. A dropout layer serves as a mask, excluding certain neurons' contributions to the subsequent layer while leaving all others alone. It is one of the regularization approaches to keep overfitting during the training phase. The final two fully connected layers are as follows: It takes the flattened layer's input and outputs a one-dimensional vector. The final layer will compute class scores for each image, resulting in a binary class [0, 1] where the normal image is represented by 0 and the tumor image is represented by 1. The sigmoid activation function is applied to generate the final output.

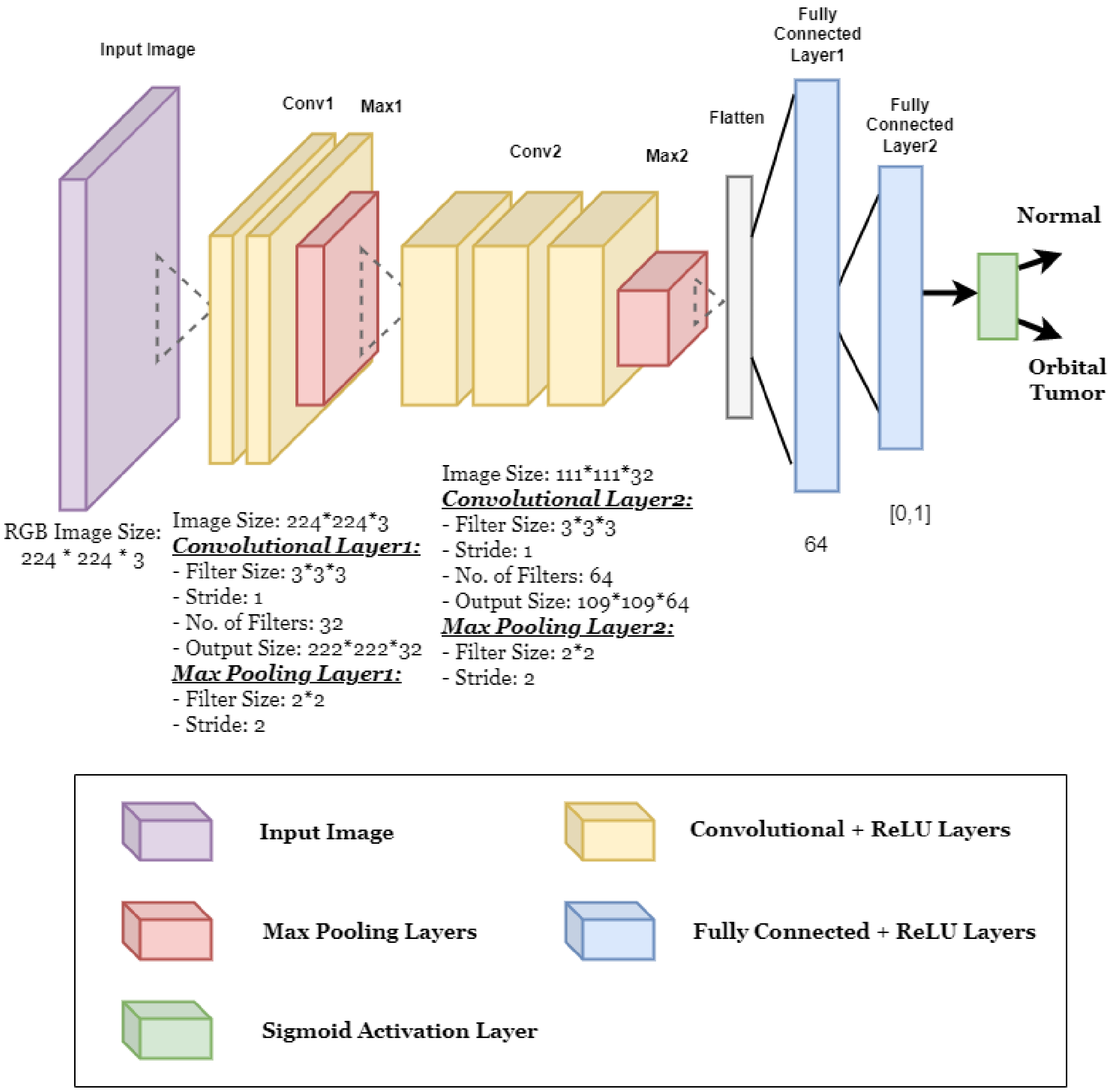

Figure. 5: The CNN Model Architecture

4. Results and Discussion

The research involved two MRI datasets: T1-weighted and T2-weighted images. The MRI T1-weighted images dataset contains 1404 MRI images, 702 of which are normal and 702 of which are tumor images. The MRI T2-weighted images dataset contains 1560 MRI images, 780 of which are normal and 780 of which are tumors. Each dataset was broken into three parts: training, validation, and testing. For this aim, 80% of all images were assigned to the training group, with the remaining images divided into the validation (10%) and testing (10%) groups. The accuracy, recall, precision, and f1-score were used to evaluate the system's performance. Table 1 displays the outcomes of our suggested system. Figure 6 depicts the model training and validation accuracy and loss results for MRI T1-weighted images across epochs, whereas Figure 7 depicts the model training and validation accuracy and loss results for MRI T2-weighted images across epochs.

Table 1 The results of our proposed CNN model

	T1-weighted images	T2-weighted images
Accuracy	95%	94%
Recall	94%	90%
Precision	95%	91%
f1-score	96%	94%

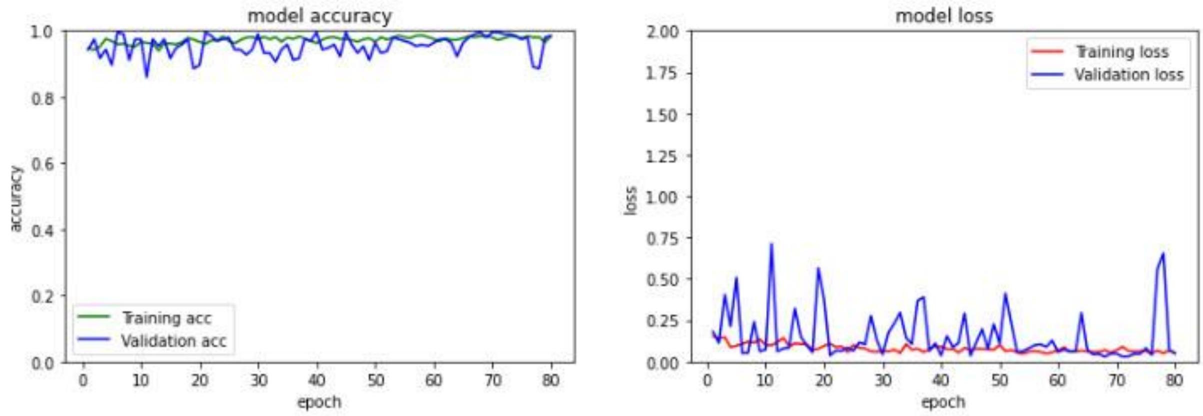

Figure. 6: The model training and validation accuracy and loss for MRI T1-weighted images

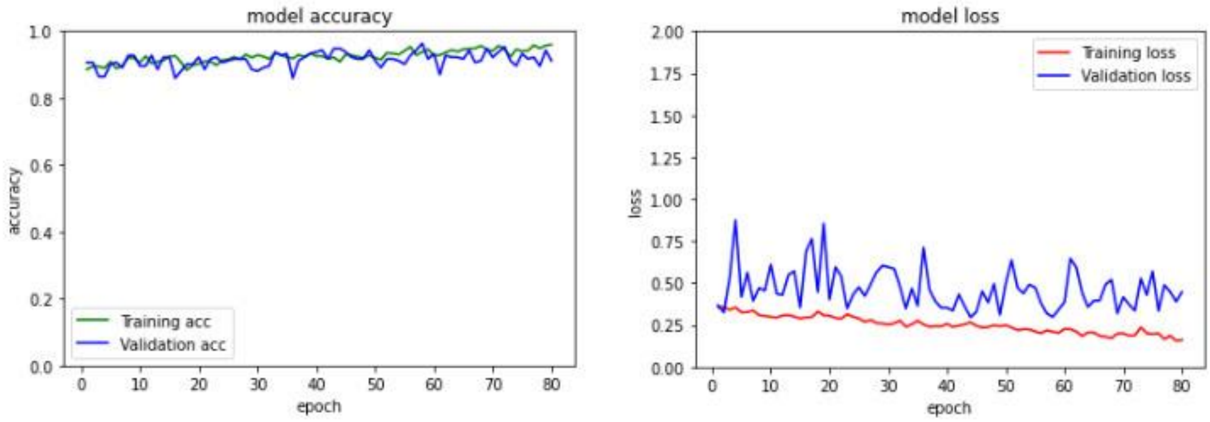

Figure. 7: The model training and validation accuracy and loss for MRI T2-weighted images

To the best of our knowledge, no previous research has been conducted to classify orbital tumors; this is the first research on this type of tumor. But there are previous studies that classified different types of eye tumors. The results are compared with the existing technique in terms of performance indices tabulated in Table 2.

The experiment results demonstrated very promising outcomes that had an accuracy of 95% for MRI T1-weighted images and an accuracy of 94% for MRI T2-weighted images. Figure 6 and 7 illustrates no overfitting between the training and validation across the epochs.

Table 2 Performance comparison with previous work

Publication	Methodology	Performance
Biswarup, et al, 2019 [14]	CNN	A recognition rate is 91.76 %
Sheshang, et al, 2022 [15]	CNN	Accuracy is 92.5%.
Parmod , et al, 2023 [18]	AlexNet ResNet50	Accuracy is 88.12% for AlexNet and 93.16% for ResNet50 algorithms.
Proposed	CNN	Accuracy is 95% for MRI T1-weighted and 94% for MRI T2-weighted images

5. Conclusion and Future Work

This research presented a novel CAD system that would support ophthalmologists to classify and detect an orbital tumor from MRI images using Convolutional Neural Networks. To enhance and improve the dataset, the following preprocessing techniques were applied: median filter, Gaussian blur filter, brightness filter, contrast filter, and edge enhance filters. Data augmentation techniques such as horizontal flipping, shifting, zooming, shearing, rescaling, resizing, and rotation manipulation were implemented to increase the model's performance and accuracy. The model was trained using two private MRI datasets: 1404 T1-weighted images and 1560 T2-weighted images. The T1-weighted image had a 95% recognition rate, whereas the T2-weighted image had a 94% recognition rate. In the future, we want to expand on this work by testing on bigger datasets to improve accuracy. In addition, we will test our model on several image types, including computed tomography, ultrasound, and histology images. We will use it to distinguish between various forms of eye malignancies, such as iris, conjunctiva, uvea, and secondary tumors.

Acknowledgement

The authors would like to thank Dr Azza Mohamed Ahmed, Professor of Ophthalmology, Faculty of Medicine, Ain Shams University for her contribution to the collection of the dataset and validation of the results.

References

1. Blandford, Alexander D., and Julian D. Perry, Classification of orbital tumors, Clinical ophthalmic oncology, Springer, Cham, 2019.
2. Kannan, Satish, Mitsuhiro Hasegawa, Yasuhiro Yamada, Tsukasa Kawase, and Yoko Kato, Tumors of the orbit: Case report and review of surgical corridors and current options, Asian Journal of Neurosurgery 14(3) (2019) 678.
3. Zhang, Li, Xuying Li, Fei Tang, Lu Gan, and Xin Wei., Diagnostic imaging methods and comparative analysis of orbital cavernous hemangioma, Frontiers in Oncology 10 (2020) 577452.
4. Vogele, Daniel, Nico Sollmann, Annika Beck, Benedikt Haggenmüller, Stefan Andreas Schmidt, Bernd Schmitz, Thomas Kapapa, Yigit Ozpeynirci, Meinrad Beer, and Christopher Kloth, Orbital Tumor - Clinical, Radiologic and Histopathologic Correlation, Diagnostics 12(10) (2022) 2376.
5. Ting, D.S.W., Pasquale, L.R., Peng, L., Campbell, J.P., Lee, A.Y., Raman, R., Tan, G.S.W., Schmetterer, L., Keane, P.A. and Wong, T.Y., Artificial intelligence and deep learning in ophthalmology, British Journal of Ophthalmology 103(2) (2019) 167-175.
6. Balyen, Lokman, and Tunde Peto., Promising artificial intelligence - machine learning - deep learning algorithms in ophthalmology, The Asia-Pacific Journal of Ophthalmology 8(3) (2019) 264-272.

7. Tayal, Akash, Jivansha Gupta, Arun Solanki, Khyati Bisht, Anand Nayyar, and Mehedi Masud, DL-CNN-based approach with image processing techniques for diagnosis of retinal diseases, Multimedia Systems 28(4) (2022) 1417-1438.
8. Du, Xue-Li, Wen-Bo Li, and Bo-Jie Hu, Application of artificial intelligence in ophthalmology, International Journal of Ophthalmology 11(9) (2018) 1555.
9. Hogarty, Daniel T., David A. Mackey, and Alex W. Hewitt, Current state and future prospects of artificial intelligence in ophthalmology: a review, Clinical & experimental ophthalmology 47(1) (2019) 128-139.
10. Kermany, Daniel S., Michael Goldbaum, Wenjia Cai, Carolina CS Valentim, Huiying Liang, Sally L. Baxter, Alex McKeown et al., Identifying medical diagnoses and treatable diseases by image-based deep learning, Cell 172(5) (2018) 1122-1131.
11. Qin, Chunli, Demin Yao, Yonghong Shi, and Zhijian Song, Computer-aided detection in chest radiography based on artificial intelligence: a survey, Biomedical engineering online 17(1) (2018) 1-23.
12. Sarvamangala, D. R., and R. V. Kulkarni, Convolutional neural networks in medical image understanding: a survey, Evolutionary Intelligence 15(1) (2022) 1-22.
13. Kugunavar, Sneha, and C. J. Prabhakar, Convolutional neural networks for the diagnosis and prognosis of the coronavirus disease pandemic, Visual computing for industry, biomedicine, and art 4(1) (2021) 1-14.
14. Ganguly, Biswarup, Shreya Biswas, Samrat Ghosh, Sabyasachi Maiti, and Snehasish Bodhak, A deep learning framework for eye melanoma detection employing convolutional neural network. In: 2019 international conference on Computer, electrical & communication engineering (ICCECE), 2019, p. 1-4. IEEE.
15. Degadwala, Sheshang, Dhairya Vyas, Harsh S. Dave, Vaishnavi Patel, and Jay N. Mehta, Eye Melanoma Cancer Detection and Classification Using CNN, In: Second International Conference on Image Processing and Capsule Networks: ICIPCN 2021, p. 489-497. Springer International Publishing, 2022.
16. Miles Research, available: http://www.milesresearch.com/main/links.htm, 2023 (accessed 30 June 2023).
17. The Eye Cancer Foundation. http://www.eyecancer.com/research/image-gallery/, 2023 (accessed 30 June 2023).
18. Kumar, Parmod, D. Suganthi, K. Valarmathi, Mahendra Pratap Swain, Piyush Vashistha, Dharam Buddhi, and Emmanuel Sey, A Multi-Thresholding-Based Discriminative Neural Classifier for Detection of Retinoblastoma Using CNN Models, BioMed Research International 2023, (2023).
19. Jemima Jeba, “Retinoblastoma dataset,” 2023, June 2023, MATLAB Central File Exchange. (https://www.mathworks.com/matlabcentral/fileexchange/99559-retinoblastoma-dataset),
20. Radiopaedia Image Bank, https://radiopaedia.org/, 2023 (accessed 1 January 2023)
21. Rezaei, Mina, Haojin Yang, and Christoph Meinel, Deep neural network with l2-norm unit for brain lesions detection, In: International Conference on Neural Information Processing, 2017, p.798-807. Springer, Cham.
22. Goodfellow, Ian, Yoshua Bengio, and Aaron Courville, Deep learning, MIT Press, 2016.
23. Shorten, Connor, and Taghi M. Khoshgoftaar, A survey on image data augmentation for deep learning, Journal of Big Data 6(1) (2019) 1-48.